



HAL
open science

Measurement of ambient aerosols in northern Mexico City by single particle mass spectrometry

R. C. Moffet, B. de Foy, L. T. Molina, M. J. Molina, A. Prather

► **To cite this version:**

R. C. Moffet, B. de Foy, L. T. Molina, M. J. Molina, A. Prather. Measurement of ambient aerosols in northern Mexico City by single particle mass spectrometry. *Atmospheric Chemistry and Physics Discussions*, 2007, 7 (3), pp.6413-6457. hal-00302766

HAL Id: hal-00302766

<https://hal.science/hal-00302766>

Submitted on 18 Jun 2008

HAL is a multi-disciplinary open access archive for the deposit and dissemination of scientific research documents, whether they are published or not. The documents may come from teaching and research institutions in France or abroad, or from public or private research centers.

L'archive ouverte pluridisciplinaire **HAL**, est destinée au dépôt et à la diffusion de documents scientifiques de niveau recherche, publiés ou non, émanant des établissements d'enseignement et de recherche français ou étrangers, des laboratoires publics ou privés.

**Single particle mass
spectrometry of
Mexico City aerosols**

R. C. Moffet

Measurement of ambient aerosols in northern Mexico City by single particle mass spectrometry

R. C. Moffet¹, B. de Foy^{2,3}, L. T. Molina^{2,4}, M. J. Molina¹, and A. Prather¹

¹University of California, San Diego, La Jolla, CA, USA

²Molina Center for Energy and the Environment (MCE²), La Jolla, d CA, USA

³Saint Louis University, Saint Louis, Missouri, USA

⁴Massachusetts Institute of Technology, Cambridge, MA, USA

Received: 18 April 2007 – Accepted: 25 April 2007 – Published: 11 May 2007

Correspondence to: K. A. Prather (kprather@ucsd.edu)

Title Page

Abstract

Introduction

Conclusions

References

Tables

Figures

◀

▶

◀

▶

Back

Close

Full Screen / Esc

Printer-friendly Version

Interactive Discussion

Abstract

Continuous ambient measurements with aerosol time-of-flight mass spectrometry (ATOFMS) were carried out in an industrial/residential section in the northern part of Mexico City as part of the Mexico City Metropolitan Area – 2006 campaign (MCMA-2006) between 7–27 March, 2006. Biomass and organic carbon (OC) particle types were found to dominate the accumulation mode both day and night. The concentrations of both organic carbon and biomass particles were roughly equal early in the morning, but biomass became the largest contributor to the accumulation mode mass from the late morning until early evening. The diurnal pattern can be attributed to aging and/or a change in meteorology. Fresh elemental carbon (EC) particles were observed during rush hour. The majority of the EC particles were mixed with nitrate, sulfate, organic carbon and potassium. Submicron particles from industrial sources in the northeast were composed of an internal mixture of Pb, Zn, EC and Cl and peaked early in the morning. A unique nitrogen-containing organic (NOC) particle type was observed, and is hypothesized to be from industrial emissions based on the temporal profile and back trajectory analysis. This study provides unique insights into the real-time changes in single particle mixing state as a function of size and time for aerosols in Mexico City. These new findings indicate that biomass burning and industrial operations make significant contributions to particles in Mexico City. These sources have received relatively little attention in previous intensive field campaigns.

1 Introduction

The Mexico City Metropolitan Area (MCMA) is a megacity that allows for a unique opportunity to study air pollution. High levels of criteria pollutants are a product of the city's high population density, meteorology, and unique geographical location. Both gas and particle phase contaminants are generated that degrade human health and affect climate and visibility. A voluminous body of literature has resulted from studies of

ACPD

7, 6413–6457, 2007

Single particle mass spectrometry of Mexico City aerosols

R. C. Moffet

Title Page

Abstract

Introduction

Conclusions

References

Tables

Figures

◀

▶

◀

▶

Back

Close

Full Screen / Esc

Printer-friendly Version

Interactive Discussion

EGU

pollutants in the MCMA, with research focusing on a wide range of topics that include health effects, gas and particle phase measurements, modeling, economics and policy (Molina, 2002; Raga et al., 2001). The basic approach has been to use Mexico City as a case study of air pollution mitigation while major advances continue to improve the regional air quality.

To help decrease particulate matter (PM) pollution in Mexico City, one needs a better understanding of the spatial and temporal variability of the sources, size distribution, and chemical composition of the ambient aerosol. Knowledge of these parameters enables well-guided strategies for decreasing the PM fraction that is suspected to be the most harmful to human health. Prior to the development of the Automatic Ambient Air Quality Monitoring Network (RAMA) measurements that began in the mid 1980s, there were very few detailed measurements of particulate matter chemical composition in Mexico City. From the late 1980's to present, Aldape, Miranda, Flores and co-workers measured PM chemical composition in Mexico City by using filters to collect PM followed by analysis with Proton Induced X-Ray Emission (PIXE) (Aldape et al., 1996a, b; Cahill et al., 1996; Flores et al., 1999; Miranda et al., 1992, 1998, 2004). Flores (1999) showed that there were increased concentrations of lead, copper and zinc in the northern (industrial) part of the city. These results were further corroborated by later results from the sampling period (Mugica et al., 2002).

In the late 1990s, as part of the Aerosol and Visibility Evaluation Research (IMADA-AVER) campaign, Chow and co-workers measured the chemical composition of $PM_{2.5}$ and PM_{10} at a variety of sites using filter based techniques while also publishing complementary results characterizing the chemical composition of fugitive dust sources (Chow et al., 2002a, b; Vega et al., 2002). Moya and co-workers examined the gas-particle equilibrium of ammonium and nitrate during the same campaign for purposes of evaluating thermodynamic models (Moya et al., 2001). They followed up those studies with size resolved measurements focusing on ammonium and sulfate from winter of 2000 to fall of 2001, but also included measurements of other cations (Moya et al., 2003). From January to February of 2003, Moya and co-workers provided a size-

Single particle mass spectrometry of Mexico City aerosols

R. C. Moffet

Title Page

Abstract

Introduction

Conclusions

References

Tables

Figures

◀

▶

◀

▶

Back

Close

Full Screen / Esc

Printer-friendly Version

Interactive Discussion

resolved characterization of inorganic species. They found an unexpectedly large concentration of K particles, which they attributed to dust from the dry lake bed of Texcoco in the northeastern part of the city (Moya et al., 2004).

The most recent and detailed studies of aerosols in Mexico City were carried out during the MCMA-2003 campaign (Baumgardner et al., 2004; Dunn et al., 2004; Jiang et al., 2005; Jimenez et al., 2004; Marr et al., 2006). Electron microscopy was used to infer the mixing state and transformation of soot particles (Johnson et al., 2005). Chemically resolved $PM_{2.5}$ mass distributions were obtained using a variety of techniques including Aerosol Mass Spectrometry (AMS), and other filter based techniques (Salcedo et al., 2006). Salcedo et al. (2006) was also able to track mass concentrations of select, non-refractory aerosol components with a higher time resolution than previously reported by Chow et al. (2002a), while showing a general agreement between the two studies. Newer source apportionment measurements during the MCMA-2003 campaign were able to classify major sources of particles including industrial emissions using factor analysis (Johnson, 2006). Industrial emissions in Johnston et al. (2006) were found to be well correlated with Na and Zn as well as other metals.

Many earlier studies of aerosol size and composition in Mexico City from 1990 to the present day were carried out as a part of major campaigns funded through an international effort (Molina, 2002). Prior to 2006, there were three major research initiatives that measured aerosol physico-chemical properties: The Mexico City Air Quality Research Initiative (MARI), IMADA-AVER and MCMA-2003. The current effort: MILAGRO (Megacity Initiative: Local and Global Research Observations) is the largest to date representing the collaboration of over 400 scientists, from more than 120 institutions. A component of MILAGRO, MCMA-2006, with cooperation from NSF, DOE and a variety of Mexican and European agencies, represents an effort to characterize boundary layer emissions within the MCMA. The single particle mass spectrometry measurements discussed herein represented a new approach for studying air quality in Mexico City and were conducted as part of MCMA – 2006. The goal of this current paper is to provide unique insights into the real-time changes in single particle mixing state as a

Single particle mass spectrometry of Mexico City aerosols

R. C. Moffet

Title Page

Abstract

Introduction

Conclusions

References

Tables

Figures

◀

▶

◀

▶

Back

Close

Full Screen / Esc

Printer-friendly Version

Interactive Discussion

function of size and time for aerosols in Mexico City.

2 Experimental

2.1 Sampling site – T0

The ATOFMS instrument was located at the Instituto Mexicano del Petroleo (IMP) in the northern part of Mexico City (19°29′23.60 N, 99°08′55.60 W). This was one of the three supersites selected for the MILAGRO measurement campaign to characterize the transport of emissions from the urban areas in the MCMA to the surrounding regions. Figure 1 shows the geographical location of the IMP site, referred as T0 (urban site). Measurements were located in a secondary structure on top of a five-story building. Sampling lines were placed >10' above the structure's roof to minimize the effects of sampling from the building ventilation exhaust ports. To the north was an 800 m high mountain, Cerro del Chiquihuite, that served to block most of the winds coming from the north. An industrialized area existed to the west, while urban areas resided to the east and south. A dry lake bed of Lake Texcoco was located to the east. A busy roadway was located on the east side of the site with traffic jams during most of the day and street vendors cooking primarily during the morning and afternoon.

2.2 ATOFMS measurements and clustering analysis

The ATOFMS is an instrument designed to measure real-time size and chemical composition of aerosols. The specific model of the instrument used in Mexico City is described in (Gard et al., 1997). The aerosols are drawn through a nozzle inlet where the gas undergoes a supersonic expansion, and the particles are accelerated to a specific terminal velocity depending on their aerodynamic size. The particle velocity is determined by measuring the time-of-flight between two 50 mW diode pumped, solid state, frequency doubled Nd:YAG lasers operating at 532 nm. The single-particle scattering

Single particle mass spectrometry of Mexico City aerosols

R. C. Moffet

Title Page

Abstract

Introduction

Conclusions

References

Tables

Figures

◀

▶

◀

▶

Back

Close

Full Screen / Esc

Printer-friendly Version

Interactive Discussion

Single particle mass spectrometry of Mexico City aerosolsR. C. Moffet

Title Page

Abstract

Introduction

Conclusions

References

Tables

Figures

◀

▶

◀

▶

Back

Close

Full Screen / Esc

Printer-friendly Version

Interactive Discussion

intensities from the two light scattering channels were acquired and saved along with the other single particle data as described in Moffet (2005) (Moffet and Prather, 2005). The particle size is then calculated from the speed using a calibration curve generated with known sizes of standard polystyrene spheres. The speed of the particle is also used to time the arrival of the particle in the ion source region of the dual-polarity time-of-flight mass spectrometer. Once the particle is in the source region, a frequency quadrupled Nd:YAG laser operating at 266 nm with a typical pulse energy of 1.2 mJ desorbs and ionizes each particle. The ATOFMS measures both the positive and negative mass spectra of each particle simultaneously.

The ATOFMS has wide dynamic range capabilities. This is accomplished by taking the two signals from the two mass spectra being measured (positive and negative ion) and splitting them into an attenuated (30 dB) and non-attenuated channel, making four signals in total. The ATOFMS was operated from 6 March 2006 to 29 March 2006. Due to damage incurred during shipment, from 6 March 2006 19:00:01 to 13 March 2006 16:00:01, the instrument was operated without the negative wide dynamic range channel. After March 2006 16:00:01, both the negative and positive mass spectra were acquired using wide dynamic range.

A total of 1.6 million particles were sized and chemically analyzed with the mass spectrometer. The typical percentage of particles producing both size and chemical information was 50%; of these particles, 88% produced both positive and negative spectra. This percentage showed little variation over the study, indicating chemical matrix effects did not play a major role (Wenzel et al., 2003). Data from the ATOFMS were imported into a Matlab database program known as YAADA (<http://www.yaada.org>). Once in the Matlab database, the particles were split into four groups: sub and super-micron having wide dynamic range and non-wide dynamic range. The 48 000 particles from the four subsets of particles were separately classified using ART-2a, a clustering algorithm (Song et al., 1999), run with a vigilance factor of 0.80 and a learning rate of 0.05. The clusters resulting from each analysis were matched to the rest of the particles in the complete dataset. In order to classify 1.4 million out of 1.6 million par-

ticles, 60 sub-micron and 200 super-micron clusters were considered (for each of the four groups) and accounted for 88% of the chemically analyzed particles. The 200 000 particles not classified made up a large number of sparsely populated clusters. The unclassified particles did not have any major temporal spikes indicating that the original number of particles given to ART-2a was sufficient. The particle clusters resulting from the ART-2a analysis were grouped by hand into 15 general particle types.

Hourly scaling functions were derived by scaling the ATOFMS data with size distribution data acquired with an aerodynamic particle sizer (APS, TSI, Inc.) using the method developed previously by our group (Qin et al., 2006). These scaled data were then used to derive mass concentrations of the specific particle classes by assuming the densities suggested by Qin et al. (2006).

3 Results and discussion

For the 3.5 weeks that the ATOFMS operated at the T0 site, unique anthropogenic particle types and mixing states were observed in northern Mexico City. These unique particle types primarily contained different metals and organic nitrogen species. The majority of particles in the accumulation mode were either identified as biomass (from meat cooking or biomass burning), or organic carbon (OC). In the coarse (super-micron) mode, inorganic dust types were found to dominate. For all particle types, hourly time series (Sect. 3.4) and chemically resolved size distributions were obtained (Sect. 3.2). Average diurnal trends indicate that industrial emissions primarily occur in the early morning and that biomass and OC make the largest contributions to aerosol mass during the early morning to late afternoon hours. To identify possible source regions, a concentration field analysis was performed by combining ATOFMS time series with stochastic Lagrangian back trajectories (Sect. 3.5).

Single particle mass spectrometry of Mexico City aerosols

R. C. Moffet

Title Page

Abstract

Introduction

Conclusions

References

Tables

Figures

◀

▶

◀

▶

Back

Close

Full Screen / Esc

Printer-friendly Version

Interactive Discussion

3.1 Mass spectral analysis of the major particle types

Overall, out of the 1.6 million particles analyzed, 88% of the particles were placed into 15 general types by hand grouping the 60 submicron and 200 supermicron clusters from the ART-2a analysis. The average mass spectra for the single particle types are displayed in Figs. 2a and b. A feature that is common to all of the particle types is that $^{46}\text{NO}_2^-$ and $^{62}\text{NO}_3^-$ are detected in the negative ion spectra, indicating a significant amount of secondary processing. Other secondary markers occur in the positive ion spectra, namely $^{18}\text{NH}_4^+$ and $^{43}\text{C}_2\text{H}_3\text{O}^+$. Fine mode particles, especially carbonaceous types, contain sulfate ($^{97}\text{HSO}_4^-$) in their negative spectra. Conversely, coarse mode particle types (AlSi, NaK, Ca Dust) often contain other different markers in their negative ion mass spectra such as $^{35}\text{Cl}^-$ and $^{79}\text{PO}_3^-$.

3.1.1 Carbonaceous particle types

OC: Organic carbon (OC) particles were one of the most abundant particle types observed during this study. These particles are similar to those detected in other ATOFMS field studies (Liu et al., 2003; Noble and Prather, 1996; Pastor et al., 2003) and vehicular source characterization studies (Sodeman et al., 2005; Toner et al., 2006). OC particles are typified by a large number of hydrocarbon envelope peaks that start with the base carbon peak $^{12n}\text{C}_n^+$. In Fig. 2a, the major hydrocarbon-containing peaks are identified as $^{27}\text{C}_2\text{H}_3^+$ and $^{43}\text{C}_2\text{H}_3\text{O}^+$. Many spectra also contain a large peak at m/z 39 (K⁺), indicating agglomeration between OC and biomass types.

Biomass: Previous ATOFMS studies have provided a solid basis for the identification of biomass particles (Guazzotti et al., 2003; Silva et al., 1999). Particles classified as biomass always have $^{39}\text{K}^+$ as one of the largest peaks in the positive ion mass spectrum. Additionally, the biomass mass spectrum contains carbon marker ions. Na^+ is more prominent in the biomass particles than it is in the other carbonaceous particle types (with the exception of the NaEC type). Particles having these chemical signatures can be emitted as a result of biomass burning or cooking operations (Silva, 2000).

Title Page

Abstract

Introduction

Conclusions

References

Tables

Figures

◀

▶

◀

▶

Back

Close

Full Screen / Esc

Printer-friendly Version

Interactive Discussion

Single particle mass spectrometry of Mexico City aerosolsR. C. Moffet

[Title Page](#)[Abstract](#)[Introduction](#)[Conclusions](#)[References](#)[Tables](#)[Figures](#)[◀](#)[▶](#)[◀](#)[▶](#)[Back](#)[Close](#)[Full Screen / Esc](#)[Printer-friendly Version](#)[Interactive Discussion](#)

NaEC: The NaEC type is characterized by elemental carbon cluster ions at spacing of 12 m/z units in both the positive and negative ion spectra. This type has a dominant $^{23}\text{Na}^+$ peak. This combination of EC and Na ions is consistent with observations in other single particle mass spectrometry measurements of heavy duty vehicle (HDV) emissions (Toner et al., 2006) and field studies (Guazzotti et al., 2001; Liu et al., 2003; Noble and Prather, 1996; Pastor et al., 2003).

ECOC: The Elemental Carbon/Organic Carbon (ECOC) type is characterized by a positive ion mass spectrum that is dominated by clusters of carbon atoms. In addition to the major elemental carbon markers, minor signals occur from organic carbon envelopes along with many of the typical OC markers.

High Mass OC: The high mass organic carbon class was made to be a separate particle type due to the presence of hydrocarbon envelopes in the positive ions extending above 100 Da. Typically these hydrocarbon envelopes have a $\Delta m/z = 14$, which is due to successive losses of a $^{14}\text{CH}_2$ group. Although not shown in the figure, the hydrocarbon envelopes can extend out to $m/z = 200$ and above. High mass negative ions have been shown in lab secondary organic aerosol (SOA) studies (Gross et al., 2006) and have been attributed to oligomeric species. Positive ion laser desorption ionization mass spectra at 266 nm with such high mass signatures are typically attributed to polycyclic aromatic hydrocarbons (PAH) (Gross et al., 2000).

Vanadium: Vanadium particles have been identified with other analytical methods as well as single particle mass spectrometry in studies of light duty vehicle (LDV) emissions (Sodeman et al., 2005), from industrial urban areas (Noble and Prather, 1996; Tolocka et al., 2004), and from coal and oil fired power plant emissions (Suarez and Ondov, 2002). Particles containing vanadium produce a very unique mass spectrum with peaks at $^{51}\text{V}^+$ and $^{67}\text{VO}^+$. Oxalate was seen in the negative mass spectrum at $m/z = 89$, having the chemical formula $^{89}\text{C}_2\text{O}_3\text{OH}^-$. Secondary sulfate and primary vanadium are a result of emissions from fossil fuel combustion. Oxalate may be from either biomass burning, or VOC oxidation followed by subsequent cloud processing (Chebbi and Carlier, 1996; Morawska and Zhang, 2002). The fraction of the oxalic acid

mass formed by cloud processing is currently a topic of research (Ervens et al., 2004; Kanakidou et al., 2005).

Nitrogen-containing organic (NOC): One of the new particle types detected in this study includes the NOC particle type. The “NOC” label is used due to the large peak at $m/z = 58$ which we hypothesize is due to $^{58}\text{C}_2\text{H}_5\text{NHCH}_2^+$ which has been identified by ATOFMS and in other laboratory studies (Angelino et al., 2001; Pitts et al., 1978). There is also a grouping of peaks at $m/z = 212\text{--}215$ of unknown identity. Although the peaks are small, they occur on almost every NOC particle detected.

3.1.2 Coarse mode particle types

NaK: Some particles are characterized by having the majority of the positive spectrum dominated by $^{23}\text{Na}^+$ or $^{39}\text{K}^+$. The negative spectrum shows nitrate $^{46}\text{NO}_2^-$ and $^{62}\text{NO}_3^-$ as the major peaks, but there is also significant signal from $^{79}\text{PO}_3^-$ and $^{35,37}\text{Cl}^-$. Coarse mode Na and K have been found to be in soil dust, biogenic material, and sea salt (Beddows et al., 2004).

AlSi: $^{27}\text{Al}^+$ was frequently found to be mixed with $^{23}\text{Na}^+$, $^{39}\text{K}^+$ and $^{35}\text{Cl}^-$. If Al was associated with silicon markers $^{60}\text{SiO}_2^-$ and $^{76}\text{SiO}_3^-$, the particle was placed in the Al/Si class. The presence of these peaks suggests that the particle was an aluminosilicate species common to mineral dust. ^7Li was another common peak seen in the positive spectrum of the Al/Si type. The peak at $m/z = 56$ could occur from $^{56}\text{Fe}^+$ or $^{56}\text{KOH}^+$; and possibly even contributions from $^{56}\text{CaO}^+$ when there is a corresponding peak at $m/z = 40$, indicating $^{40}\text{Ca}^+$.

Ca: At $m/z = 40$ $^{40}\text{Ca}^+$ stands out as the largest peak in the positive ion spectrum accompanied by smaller peaks at $m/z = 56$ and 57 due to $^{56}\text{CaO}^+$ and $^{57}\text{CaOH}^+$. Previous studies have described the ability of CaCO_3 dust to react with nitric acid to form $\text{Ca}(\text{NO}_3)_2$ (Krueger et al., 2004; Laskin et al., 2005). It is likely that the calcium dust shown herein has undergone this reaction as indicated by the negative ion mass spectrum which shows intense markers for nitrite and nitrate at $^{46}\text{NO}_2^-$ and $^{62}\text{NO}_3^-$.

Title Page

Abstract

Introduction

Conclusions

References

Tables

Figures

◀

▶

◀

▶

Back

Close

Full Screen / Esc

Printer-friendly Version

Interactive Discussion

Minor peaks are seen in the positive spectrum at 24 and 27, likely due to Mg and Al, respectively.

3.1.3 Metal-rich particles

PbZn: Zn is one of the largest contributors to the positive ion spectrum occurring at $m/z = +64, +66, +67$ and $+68$. Often internally mixed with Zn, Pb shows up at $m/z = +206, +207,$ and $+208$. Other major peaks in the positive spectrum were $^{23}\text{Na}^+$ and $^{39}\text{K}^+$. It has been observed in other studies that Pb, Zn and Na were associated with the industrial areas in northern Mexico City (Chow et al., 2002a; Flores et al., 1999; Johnson et al., 2006; Miranda et al., 1994). In addition to $^{46}\text{NO}_2^-$ and $^{62}\text{NO}_3^-$, $^{35}\text{Cl}^-$ was one of the most abundant markers in the negative ion spectrum. In general, zinc and lead chlorides have relatively low boiling points (732°C and 950°C respectively), and their precursors may be present in high temperature combustion sources such as waste incinerators (Hu et al., 2003; Olmez et al., 1988; Ondov and Wexler, 1998). Upon cooling, these compounds will condense into the solid phase, forming submicron Cl-containing particles.

PbNa: It was common for Pb to occur without Zn, so the Pb/Na particles were separated to highlight this difference in mixing state. The Pb/Na type has Pb as the major transition metal marker. As for the PbZn type, Na was typically the largest peak in the positive ion mass spectrum, followed by potassium. Another similarity between Pb/Na and Pb/Zn is the appearance of the $^{35}\text{Cl}^-$ peak in the negative mass spectrum.

Other metal types: The other minor particle types that account for less than 1.3% of the total particles analyzed during the study were given the following labels: Cu, Fe, and miscellaneous metals (MiscMetals). The Cu particle type typically was mixed with EC, Pb, Cl, Na and K. MiscMetals contained a combination of different particle types containing various elements including Mg, Mn, Ti, and Ag.

Single particle mass spectrometry of Mexico City aerosols

R. C. Moffet

Title Page

Abstract

Introduction

Conclusions

References

Tables

Figures

◀

▶

◀

▶

Back

Close

Full Screen / Esc

Printer-friendly Version

Interactive Discussion

3.2 Chemically resolved particle size distributions

Figure 3 presents the average mass distribution of the major particle types detected with the ATOFMS during the MCMA-2006. This size distribution was determined by scaling the ATOFMS data to the APS using a separate density for each particle class to transform the volume distribution into a mass distribution. In this study, we used the density value of 1.9 g/cm^3 for carbonaceous particles, 2.7 g/cm^3 for dust particles, 1.9 g/cm^3 for Na-rich salt particles, 2.0 g/cm^3 for biomass emission particles and EC rich particles, and 1.9 g/cm^3 for the rest of the particle types. This follows the method developed by Qin et al. (2006). By integrating the size distribution shown in Fig. 3, we determine the average $\text{PM}_{2.5}$ mass to be $43.5 \mu\text{g/m}^3$. This mass concentration is close to the value of $44.34 \mu\text{g/m}^3$ obtained by Chow et al. (2002a, b) at the Xalostoc site (XAL in Fig. 1; close to T0), as well as that obtained at the RAMA site ($38.1 \mu\text{g/m}^3$) during the same time period as the current measurements. The RAMA site was located 1 km away from the T0 site.

With the exception of the high mass OC type, which peaked around $1 \mu\text{m}$, carbonaceous particle types are typically located in the accumulation mode between 0.1 and $1 \mu\text{m}$, whereas the super-micron coarse mode particles were inorganic dust and salt particles as seen in previous ATOFMS studies (Noble and Prather, 1996). The high mass OC type may occur at larger sizes due to the higher degree of chemical aging or fog/cloud processing these particles have undergone. Given that this particle type typically peaked at night when the relative humidity was high, this is likely the case (Qin and Prather, 2006).

The lead and zinc types have interesting size characteristics: the PbNa particle type is primarily supermicron, whereas the PbZn particle type occurs at smaller sizes with a mode at about 850 nm . If these particles were formed by condensation, this size characteristic may be due to different concentrations and physical properties of the vapor. Vanadium particles occur primarily in the submicron portion of the size distribution. Based on their size, the submicron metals are most likely a result of combustion

Title Page

Abstract

Introduction

Conclusions

References

Tables

Figures

⏪

⏩

◀

▶

Back

Close

Full Screen / Esc

Printer-friendly Version

Interactive Discussion

processes.

3.3 Analysis of mixing state using the peak search method

In addition to the cluster analysis presented above, a separate analysis involving a peak search method was employed to highlight trends in the aerosol mixing state of the various particle types. A series of markers were selected to represent the different primary and secondary species. The m/z values used for primary and secondary species are shown in Tables 1 and 2. All ion intensities were set to be above or equal to an absolute peak area (≥ 100 units) that is just above the noise level (< 50). To see which of the selected markers were associated with the various particle types, the particles with the species defined in Tables 1 and 2 were intersected with the major particle types derived from the ART-2a clustering analysis (Sect. 3.1). Figures 3 and 4 show the results of these intersections, where the color scale represents the fraction of particles of each major type (y-axis) associated with a particular marker (x-axis).

3.3.1 Mixing state of secondary species

The presence of secondary species on the various particle types (Fig. 4) provides an indication of the type of chemical processing the particles have undergone in the atmosphere. The key question is: are there differences in the associations of the major secondary species (e.g. sulfate, nitrate, and ammonium) with each of the major particle types? For instance, the EC and NOC types contain the fewest particles with ammonium, nitrate and sulfate, indicating that they may be freshly emitted. As these particles age through condensation and coagulation, they can accumulate other markers to become other particle types such as OC, ECOC and even biomass. Ammonium is seen to be constrained mainly to the submicron ECOC and OC types, whereas coarse mode particle types that contain NH_4^+ are mainly limited to the AISi and Cu types. For the AISi type, the NH_4^+ does not necessarily come from the atmosphere because it is common to find NH_4^+ in soils (Schlesinger and Hartley, 1992), and therefore may not be indicative

Single particle mass spectrometry of Mexico City aerosols

R. C. Moffet

Title Page

Abstract

Introduction

Conclusions

References

Tables

Figures

◀

▶

◀

▶

Back

Close

Full Screen / Esc

Printer-friendly Version

Interactive Discussion

of aging in this particle type.

Inorganic nitrogen species, such as NO_2 and NO_3 , mostly occur on primary inorganic particles such as dust. However, more than 50% of the fine carbonaceous particles are associated with NO_2 and NO_3 , and show nitrate is often associated with fine mode particles. Differences in abundance are most likely due to preferential partitioning of the NO_2/NO_3 to the coarse mode particle types (size distribution presented in Sect. 3.2). This is because of the competition between nitrate and sulfate for surface area. Since sulfate is non-volatile, it remains on the smaller particles (limited by gas diffusion), whereas the more volatile ammonium nitrate can evaporate from the smaller particles (Kelvin effect) and condense on coarse mode particles (Bassett and Seinfeld, 1984).

The Pb/Na, Cu, and Pb/Zn particle types are more strongly associated with NO_2/NO_3 compared to any other particle class. The Pb/Zn type is primarily a fine mode particle type, and it is unusual for particles in this size range to be so strongly associated with nitrate. Given that these industrial metal types are likely to be freshly emitted, this is an indicator that these particle classes are emitted with an air mass that contains large amounts of NO that reacted to form particulate nitrate. It is likely the NO_x displaced the Cl that was originally in the particles.

The organic carbon markers used to highlight mixing with other particle types were chosen to be $^{43}\text{C}_2\text{H}_3\text{O}^+$ and $\text{C}_2\text{O}_3\text{OH}^-$ (oxalate). It is apparent that $^{43}\text{C}_2\text{H}_3\text{O}$ is mainly associated with the fine mode particles but occurs in over 40% of the supermicron particles (with the exception of the PbNa type). This organic carbon likely comes from secondary reactions and gas-to-particle conversion. The oxalate marker is an indicator of the presence of oxalic acid. Oxalic acid may be emitted as a part of vehicle exhaust and biomass burning (Chebbi and Carlier, 1996; Falkovich et al., 2005; Kawamura and Kaplan, 1987) but is most commonly formed through secondary processes including photochemistry followed by condensation, fog processing or aerosol surface reactions (Blando and Turpin, 2000; Faust, 1994; Kawamura and Ikushima, 1993; Yao et al., 2002). Oxalate is associated with biomass and vanadium types, as shown in Fig. 4, where 37 and 45% of the particles in these classes contain the oxalate marker,

Single particle mass spectrometry of Mexico City aerosols

R. C. Moffet

Title Page

Abstract

Introduction

Conclusions

References

Tables

Figures

◀

▶

◀

▶

Back

Close

Full Screen / Esc

Printer-friendly Version

Interactive Discussion

respectively.

3.3.2 Mixing state of primary species

A marker for EC, $^{36}\text{C}_3$, was chosen to highlight the distribution of carbon – especially in the non-carbonaceous particle types. This marker can come from secondary species as well, but is more commonly detected in primary particles. In Fig. 5, it is seen that the PbZn and Cu types are mixed with EC. This result, combined with the predominately fine mode size distribution (Fig. 3), provides further evidence that the PbZn and Cu particles are products of high temperature combustion. While $^{36}\text{C}_3$ can be used to identify particle classes that are internally mixed with EC, ^{40}Ca can be used to identify unique sources of EC. Source studies indicate that particles containing both Ca and EC are primarily associated with heavy duty vehicle emissions (Toner et al., 2006). The mixing of elemental carbon with Ca is observed by searching for the typical EC markers together with Ca (CaEC). From Fig. 5, it is apparent that about 50% of the EC is associated with Ca, suggesting diesel vehicles produce a substantial fraction of EC/soot in this region.

Chlorine (m/z –35 and –37) is mainly associated with the inorganic particle types. This is supported by Fig. 5 which shows a strong degree of internal mixing between metals, K, Na and Cl. Cl is also strongly associated with the AlSi type and moderately associated with the NaK and Ca dust particle types. For Ca dust, there is much less Na and K associated with Cl compared to the other inorganic particle classes. A secondary source of Cl is HCl, which can be formed by heterogeneous displacement when primary particles composed of NaCl, KCl, PbCl_2 , or ZnCl_2 react with acidic (i.e. HNO_3 or H_2SO_4) gases. The resulting HCl can then partition to other particles. This suggests that for the metals and AlSi dust, the Cl is primary and for the Ca dust, the Cl is secondary. It has been shown in previous studies that the mixing between Cl and Ca is due mainly to secondary processing by HCl gas (Sullivan et al., 2007).

In Fig. 5, K particles are present in both the coarse and fine mode particles, whereas Na particles appear to be constrained mainly to the coarse mode. Caution is necessary

Title Page

Abstract

Introduction

Conclusions

References

Tables

Figures

◀

▶

◀

▶

Back

Close

Full Screen / Esc

Printer-friendly Version

Interactive Discussion

when interpreting this result because of the interference of ^{39}K with organic markers (e.g. $^{39}\text{C}_3\text{H}_3^+$). This may explain why a large fraction of the organic carbon particles appear to contain K. On the other hand, it is likely that organic particles also contain K, given the high relative intensity of the K ion peak. Biomass particles are a prime example of a submicron particle type that definitely contains K and organic carbon as an internal mixture. Comparison of the OC Art-2a clusters from Mexico City and Riverside, CA reveals that the peak at $m/z=39$ makes a larger contribution to Mexico City particles, indicating biomass represents a more significant source in Mexico City.

3.4 Temporal characteristics of single particle types

The temporal characteristics of the single particle types can provide a great deal of insight into the origin of the particles. In this section, the temporal profiles for sub- and super-micron particle types are described in detail. Three major events are labeled on the temporal profiles shown in Fig. 6. The first event (E1) was a large dust event where the PM_{10} concentration exceeded 1 mg/m^3 . The second event (E2) was a holiday weekend and the third event (E3) was a heavy rain event. Figure 7 shows an average diurnal cycle of scaled mass concentrations representing the average of 19 days for the study.

3.4.1 Temporal profile of the entire study

Examining the study as a whole, major features in the overall submicron temporal trends (Fig. 6a) show sharp spikes of metal and nitrogen organic carbon (NOC) particles. Frequently the metal and NOC classes peaked in the morning, usually with relatively short spikes compared with the trends of the other particle classes (organics, biomass etc). This feature suggests that the source of these particles is local. The total $\text{PM}_{2.5}$ mass concentrations during these early morning spikes were typically around $50\text{ }\mu\text{g/m}^3$ at the La Villa RAMA site. The weekend event (E2) showed lower contributions from the metal and NOC types, indicating these particles may be associated

Single particle mass spectrometry of Mexico City aerosols

R. C. Moffet

Title Page

Abstract

Introduction

Conclusions

References

Tables

Figures

◀

▶

◀

▶

Back

Close

Full Screen / Esc

Printer-friendly Version

Interactive Discussion

with industry. After the rain event (E3), the fractional contribution from the biomass decreased while OC, NOC, and metal particles increased. This trend continued for the rest of the measurement period, during which evening rain events occurred on a regular basis. Overall, the submicron classes exhibited a fairly strong diurnal behavior which will be examined further in Sect. 3.4.2.

Figure 6b shows the temporal profiles of the major supermicron particle types. There was one particularly large dust event caused by strong winds on 16 March 2006 beginning at 16:00 CST (E1) during which the measured PM_{10} exceeded 1 mg/m^3 at the San Agustin and Xalostoc RAMA sites (near the dry lake bed Texcoco, SAG and XAL in Fig. 1) and almost $700 \mu\text{g/m}^3$ at the La Villa RAMA site closest to T0. The wind blew from these sites towards the west in the direction of T0. Our results show that the Na/K and Al/Si particle types dominated the chemical composition for this time period, thus indicating that the dry lake bed and fugitive sources nearby are major contributors to these particle types. This is consistent with the observations of Chow et al. (2002a and b), who found concentrations of Al, Si, K, and Na to be highest around the SAG and XAL sites compared to other sites around the city.

3.4.2 Average diurnal trends

Figure 7 shows the average diurnal trends for the most abundant submicron particle classes. Metal and NOC particles reached their highest concentrations in the early morning hours between midnight and 10:00 a.m. The most dominant particle types in the early morning (from 03:00–8:00 a.m.) were the OC and biomass particle classes. As the day continued, the relative proportion of ECOC and biomass increased. Biomass was the most abundant particle class from 08:00 a.m. to 05:30 p.m. Frequently, in the late afternoon, numerous fires were observed on the periphery of the city. In the late evening into the morning, the concentration of the OC particle types increased compared to the other classes. This may be due to increased gas-to-particle phase partitioning of OC as the temperature decreased, or due to less dilution caused by a lower boundary layer. If the latter were true, this would indicate that more of the

Single particle mass spectrometry of Mexico City aerosols

R. C. Moffet

Title Page

Abstract

Introduction

Conclusions

References

Tables

Figures

◀

▶

◀

▶

Back

Close

Full Screen / Esc

Printer-friendly Version

Interactive Discussion

OC particles were retained within the basin at night (Qin and Prather, 2006).

Although it appears that biomass particles are the major source of particulate mass in the afternoons, one must use caution when interpreting this result. In the afternoon, there is more secondary organic carbon coating all of the particle classes – including the biomass class. Furthermore, coagulation can also cause a great deal of external mixing on a timescale of about 12 h (Jacobson, 2002). Because the ATOFMS has a high sensitivity to K, it is likely that if an OC particle coagulated with a biomass particle, the resulting particle would be classified as a biomass particle. Therefore, the ATOFMS would see more biomass and less OC particles in the late afternoon. On the other hand, the flow conditions in the afternoon were much different than in the morning and the relative increase in biomass particles may be indicative of influences from different sources. This aspect will be discussed further in the following section using a back trajectory analysis.

Elemental carbon showed a bimodal diurnal temporal profile with the largest temporal peak at 7:30 a.m. and the second mode occurring at 11:30 a.m. at the same time as the total mass concentration peaked. According to Fig. 8, the EC particles sampled during the early morning peak had smaller aerodynamic diameters (number distribution mode = $0.20 \mu\text{m}$) than those sampled at the later peak (number distribution mode = $0.38 \mu\text{m}$). In Fig. 8, it is also shown that the EC particles sampled later in the day had more ion intensity from NO_3^- , NH_4^+ , $\text{C}_3\text{H}_3\text{O}^+$, and K^+ . With the exception of K^+ , these markers are indicative of secondary photochemical processing. Early morning EC particles had more intensity from $^{12n}\text{C}_n^-$ clusters and sulfates in the negative ions as well as more intensity from Na^+ and Ca^+ in the positive ion mass spectrum. Most of these markers indicate primary species emitted with the elemental carbon particles. Based on these facts, it can be concluded that the early morning peak of EC is comprised of more freshly emitted particles than the EC particles which peak later in the day. In addition, the fact that the EC particles sampled later in the day have more K^+ signal indicates that a different source of EC particles begins to have a larger influence as the day progresses, or that they have undergone coagulation with K containing particles.

Single particle mass spectrometry of Mexico City aerosols

R. C. Moffet

Title Page

Abstract

Introduction

Conclusions

References

Tables

Figures

◀

▶

◀

▶

Back

Close

Full Screen / Esc

Printer-friendly Version

Interactive Discussion

3.5 Back trajectory analysis

A Concentration Field Analysis (Seibert, 1994) was carried out using back-trajectories from the FLEXPART model (Stohl et al., 2005). To accomplish this, 100 stochastic particles are released from T0 every 2 h and tracked for 3 days. All the positions of the particles every hour are summed into a gridded field indicating the source region of the air mass at each release time. These gridded fields, called Residence Time Analyses, are then multiplied by the ATOFMS normalized particle counts at the release site and summed over the entire campaign. Potential source regions are highlighted by normalizing with the sum of the unscaled residence time analysis. The method was used to analyze data from the MCMA-2003 field campaign (de Foy, 2006a). Analysis of CO data showed that the method was able to correctly identify urban emissions and analysis of SO₂ data identified possible impacts of the Tula industrial complex. This analysis was performed for each of the fifteen particle types seen during MCMA-2006; the results of this analysis are shown in Figs. 8–10. For particle types with only a few sharp peaks, a back trajectory corresponding to peak concentrations is shown.

The wind fields for the trajectories were simulated using the MM5 model with modifications for the land surface (de Foy and Molina, 2006c). Additional modifications were made to the simulation procedure (de Foy et al., 2006b). These include finer and larger domains with 92×116, 91×145 and 97×97 cells at 27, 9 and 3 km resolution respectively and 41 sigma levels in the vertical, as well as corrections to the sea surface latent heat fluxes.

3.5.1 Spatial distribution of industrial emissions

The T0 site is located in the heart of the industrial sector of the MCMA. As a result, a large fraction of the particles detected at the T0 site are expected to be from local industrial emissions. Typically, local point sources emit pollutants over short timescales. Such pollutant spikes were discussed in Sect. 3.4.1 for the metal and NOC particle types; therefore it is likely that these particle types are from local industry. For the NOC

Single particle mass spectrometry of Mexico City aerosols

R. C. Moffet

Title Page

Abstract

Introduction

Conclusions

References

Tables

Figures

◀

▶

◀

▶

Back

Close

Full Screen / Esc

Printer-friendly Version

Interactive Discussion

type, this is verified by looking at the FLEXPART back trajectory shown in Fig. 9 for the largest NOC spike occurring at 09:00 a.m. on 15 March, 2006. This figure indicates that flow was stagnant during this peak in NOC emissions, and thus the source was most likely local. Similar flow conditions were observed during other periods of the study when the NOC particle type was most abundant.

From Fig. 7, one can see that the peak of PbNa and PbZn types occurred from midnight to about 10:00 (CST). The concentration field analysis in Fig. 9 indicates source regions north of T0 for PbZn, as well as for PbNa (not shown). Concentrations of Pb and Zn in northern Mexico City have been historically high compared to other regions of Mexico City (Chow et al., 2002b). There is evidence for transport of Na and Zn particles from the northern to southern parts of the city, as Johnson et al. (2006) have shown. At the same site, Salcedo et al. (2006) noticed sharp spikes of particulate Cl in the early morning hours. In this study, we observe early morning spikes of chloride as well, and show that it is internally mixed with Pb, Zn, Na and K. Johnson et al. attributed the Na and Zn to an industrial source in their factor analysis, and Salcedo et al. suggested that most of the Cl was present as NH_4Cl . The results obtained herein show that all Na, Cl, and Zn are likely industrial and internally mixed within the same particles (Fig. 5). The speciation of Cl does not necessarily have to be exclusively NH_4Cl because NaCl, KCl, ZnCl_2 or PbCl_2 are also possible. For all of these species, displacement of Cl by NO_3 explains the strong association of the metal particle classes with NO_2/NO_3 .

3.5.2 Spatial trends of carbonaceous particle types

Carbonaceous particle types in Mexico City are expected to be produced by a variety of urban and regional sources, both primary and secondary. The concentration field analysis shown in Fig. 10 for the OC particle type shows that these particles originated from all across the basin. The EC particle type shows more intensity close to T0 and in the northwest. Because the EC particle type represents a freshly emitted particle type and also because concentrations are highest when winds are weak and variable, the

Single particle mass spectrometry of Mexico City aerosols

R. C. Moffet

Title Page

Abstract

Introduction

Conclusions

References

Tables

Figures

◀

▶

◀

▶

Back

Close

Full Screen / Esc

Printer-friendly Version

Interactive Discussion

Concentration Field Analysis does not indicate a preferred source region. EC particles coming from the north may be due to combustion operations or other industrial operations in the north. Biomass particles show a strong correlation with flow through the gap in the mountains to the southeast of the city – a region where large fires occurred.

5 This type of flow usually occurs in the afternoon when the biomass particles peaked and is associated with vertical advection and basin venting (de Foy et al., 2005; de Foy et al., 2006c). There is also slightly more source strength for the biomass particles near the hillsides of the basin. This may be due to the fact that there were frequently numerous small fires on these hills that were used to clear fields for the upcoming crop
10 season. Lastly, vanadium particles are also correlated with the gap flow from the south with a smaller signature from the north-northwest. Johnson et al. (2006) had found a single vanadium peak time period during the MCMA-2003 that was strongly correlated with SO₂ and back-trajectories from the Tula complex. During MCMA-2006, there were half a dozen peaks in the vanadium types in addition to substantial diurnal and day-
15 to-day variations. Some of the peaks are associated with SO₂ and trajectories from the north, while others are associated with weak and variable winds followed by the strong gap flow sweeping through the basin. At this time, it is unknown whether there are any large sources of vanadium particles in the MCMA. Some of the major sources that burn fuel-oil are located in the north, where Fig. 10 shows a mild influence from
20 the vanadium particle type.

3.5.3 Spatial trends in coarse mode particle types

The concentration field analysis from the coarse (super-micron) mode particle types is shown in Fig. 11. AlSi, Ca and Fe dust all had similar spatial footprints where the highest concentration events correlated well with the flow from the northwest near the
25 Tula region. For the Ca type, this would be consistent with the fact that the cement plants in that region emit dust with high concentrations of Ca (Vega et al., 2001). The Fe particle type had slightly more influence from the northwest than did the AlSi or Ca types. The NaK particle type was significantly different from any other coarse mode

Single particle mass spectrometry of Mexico City aerosols

R. C. Moffet

Title Page

Abstract

Introduction

Conclusions

References

Tables

Figures

⏪

⏩

◀

▶

Back

Close

Full Screen / Esc

Printer-friendly Version

Interactive Discussion

particle type, showing more contributions from the east to northeast. The dry lake bed Texcoco is located in the east, and has been historically correlated with increased quantities of Na and K compared to the rest of Mexico City. Also, the NaK particle type was far more distributed spatially than the other coarse mode particle types. It is also possible that the NaK type contains contributions from vegetative detritus and biomass burning, thus providing a possible explanation for its broad spatial distribution and stronger southerly signature.

4 Conclusions

ATOFMS observations during MCMA-2006 provide chemical mixing state measurements with high temporal and size resolution. A new nitrogen-containing organic (NOC) particle type was detected, and lead particles internally mixed with Zn and Cl were also frequently observed. Both of these particle types peaked in the morning hours and were likely the result of industrial emissions. Given the spatial and temporal characteristics of particles with the PbZnCl mixing state, these particles are directly associated with the source of early morning particulate Cl. Furthermore, these same metal particles are likely associated with the source of high Pb and Zn concentrations in the north as seen in previous investigations. These particles and their chemistry will be the subject of a forthcoming paper.

The most abundant particle types seen in the MCMA include biomass and other carbonaceous types for the submicron size range, and dust and inorganic types for the coarse (super-micron) mode. The mixing of these different particle types with secondary species was analyzed in further detail using a peak searching method. Organic carbon was found to be on almost 50% of the coarse mode dust types, while 45% of the biomass and 37% of the vanadium particles were associated with the oxalate ion. It was determined that 58% of the EC particles and 73% of the ECOC particles contained sulfate. This indicates that these freshly emitted particles contain a significant amount of other inorganic components as a result of the source and of secondary chemical

Single particle mass spectrometry of Mexico City aerosols

R. C. Moffet

Title Page

Abstract

Introduction

Conclusions

References

Tables

Figures

◀

▶

◀

▶

Back

Close

Full Screen / Esc

Printer-friendly Version

Interactive Discussion

processing.

A temporal analysis of the different particle types gives insight into the possible sources and transformations of the particles. Distinct diurnal variations for the OC and biomass particle types were observed with the Biomass and OC present as the most abundant particle classes in the early morning, then after 10:00 CST, biomass particles took over as the most concentrated carbonaceous particle class. This suggests that either transport and/or aging processes served to transform the chemical composition of the carbonaceous particles. After 18:00 CST, OC particles start to increase in concentration while biomass particles decrease. This diurnal variation has a potential to serve as a “clock” of the aging and transport characteristics of the aerosol in the heart of the MCMA, thus providing a timescale by which measurements can be compared with models. These temporal profiles provided by the ATOFMS were used, together with meteorological modeling to provide source regions for the major particle types. Knowledge gained from this analysis will ultimately be combined with emissions inventories for the MCMA to give the most likely sources for each of the major particle types.

Acknowledgements. This field campaign is the collaborative effort of a large number of participants with the support of multi-national agencies. The authors would like to thank G. Sosa, P. Sheehy, R. Volkamer, J. L. Jimenez, and K. Docherty for their help and guidance during the MCMA-2006 field study. R. Sanchez overcame the location problems of our digitizers. R. Osborne and D. Collins helped organize and consolidate the shipment of equipment into Mexico as well as providing APS data. T. Perez and R. Cepeda provided much needed and timely logistical support. R. Ramos graciously provided gas phase and PM data from the RAMA monitoring network. We thank NSF for funding under ATM-0511803 and ATM-0528227. We also thank DOE for funding under DE-FG02-0563980.

References

Aldape, F., Flores, J., Diaz, R. V., and Crumpton, D.: Upgrading of the PIXE system at ININ (Mexico) and report on elemental composition of atmospheric aerosols from 1990 in the

6435

ACPD

7, 6413–6457, 2007

Single particle mass spectrometry of Mexico City aerosols

R. C. Moffet

Title Page

Abstract

Introduction

Conclusions

References

Tables

Figures

◀

▶

◀

▶

Back

Close

Full Screen / Esc

Printer-friendly Version

Interactive Discussion

EGU

Single particle mass spectrometry of Mexico City aerosols

R. C. Moffet

Title Page

Abstract

Introduction

Conclusions

References

Tables

Figures

◀

▶

◀

▶

Back

Close

Full Screen / Esc

Printer-friendly Version

Interactive Discussion

ZMCM, Nucl. Instrum. Methods Phys. Res., Sect. B, 109, 459–464, 1996a.

Aldape, F., Flores, J., Garcia, R., and Nelson, J. W.: PIXE analysis of atmospheric aerosols from a simultaneous three site sampling during the autumn of 1993 in Mexico City, Nucl. Instrum. Methods Phys. Res., Sect. B, 109, 502–505, 1996b.

5 Angelino, S., Suess, D. T., and Prather, K. A.: Formation of aerosol particles from reactions of secondary and tertiary alkylamines: Characterization by aerosol time-of-flight mass spectrometry, Environ. Sci. Technol., 35(15), 3130–3138, 2001.

Bassett, M. E. and Seinfeld, J. H.: Atmospheric equilibrium-model of sulfate and nitrate aerosols 2: Particle-size analysis, Atmos. Environ., 18(6), 1163–1170, 1984.

10 Baumgardner, D., Raga, G. B., and Muhlia, A.: Evidence for the formation of CCN by photochemical processes in Mexico City, Atmos. Environ., 38(3), 357–367, 2004.

Beddows, D. C. S., Donovan, R. J., Harrison, R. M., Heal, M. R., Kinnersley, R. P., King, M. D., Nicholson, D. H., and Thompson, K. C.: Correlations in the chemical composition of rural background atmospheric aerosol in the UK determined in real time using time-of-flight mass spectrometry, J. Environ. Monitor., 6(2), 124–133, 2004.

15 Blando, J. D. and Turpin, B. J.: Secondary organic aerosol formation in cloud and fog droplets: a literature evaluation of plausibility, Atmos. Environ., 34(10), 1623–1632, 2000.

Cahill, T. A., Morales, R., and Miranda, J.: Comparative aerosol studies of Pacific Rim cities – Santiago, Chile (1987); Mexico City, Mexico (1987–1990); and Los Angeles, USA (1973 and 1987), Atmos. Environ., 30(5), 747–749, 1996.

20 Chebbi, A. and Carlier, P.: Carboxylic acids in the troposphere, occurrence, sources, and sinks: A review, Atmos. Environ., 30(24), 4233–4249, 1996.

Chow, J. C., Watson, J. G., Edgerton, S. A., and Vega, E.: Chemical composition of PM_{2.5} and PM₁₀ in Mexico City during winter 1997, Sci. Total Environ., 287(3), 177–201, 2002a.

25 Chow, J. C., Watson, J. G., Edgerton, S. A., Vega, E., and Ortiz, E.: Spatial differences in outdoor PM₁₀ mass and aerosol composition in Mexico City, Journal of the Air and Waste Management Association, 52(4), 423–434, 2002b.

de Foy, B., Caetano, E., Magana, V., Zitacuaro, A., Cardenas, B., Retama, A., Ramos, R., Molina, L. T., and Molina, M. J.: Mexico City basin wind circulation during the MCMA-2003 field campaign, Atmos. Chem. Phys., 5, 2267–2288, 2005,
<http://www.atmos-chem-phys.net/5/2267/2005/>.

30 de Foy, B., Clappier, A., Molina, L. T., and Molina, M. J.: Distinct wind convergence patterns in the Mexico City basin due to the interaction of the gap winds with the synoptic flow, Atmos.

- Chem. Phys., 6, 1249–1265, 2006a.
- de Foy, B., Lei, W., Zavala, M., Volkamer, R., Samuelsson, J., Mellqvist, J., Galle, B., Martinez, A. P., Grutter, M., and Molina, L. T.: Modelling Constraints on the emission inventory and on vertical diffusion for CO and SO₂ in the Mexico City Metropolitan Area using Solar FITR and zenith sky UV spectroscopy, *Atmos. Chem. Phys. Discuss.*, 6, 6125–6181, 2006b.
- de Foy, B. and Molina, L. T.: MODIS Land Surface Parameters for Improved MM5 Simulations in the Mexico City basin during the MILAGRO Field Campaign, in 7th Annual WRF User's Workshop, Boulder, Colorado, 2006.
- de Foy, B., Varela, J. R., Molina, L. T., and Molina, M. J.: Rapid ventilation of the Mexico City basin and regional fate of the urban plume, *Atmos. Chem. Phys.*, 6, 2321–2335, 2006c.
- Dunn, M. J., Jimenez, J. L., Baumgardner, D., Castro, T., McMurry, P. H., and Smith, J. N.: Measurements of Mexico City nanoparticle size distributions: Observations of new particle formation and growth, *Geophys. Res. Lett.*, 31(10), L10102, doi:10.1029/2004GL019483, 2004.
- Ervens, B., Feingold, G., Frost, G. J., and Kreidenweis, S. M.: A modeling study of aqueous production of dicarboxylic acids: 1. Chemical pathways and speciated organic mass production, *J. Geophys. Res. Atmos.*, 109(D15), D15205, doi:10.1029/2003JD004387, 2004.
- Falkovich, A. H., Graber, E. R., Schkolnik, G., Rudich, Y., Maenhaut, W., and Artaxo, P.: Low molecular weight organic acids in aerosol particles from Rondonia, Brazil, during the biomass-burning, transition and wet periods, *Atmos. Chem. Phys.*, 5, 781–797, 2005, <http://www.atmos-chem-phys.net/5/781/2005/>.
- Faust, B. C.: Photochemistry of Clouds, Fogs, and Aerosols, *Environ. Sci. Technol.*, 28(5), A217–A222, 1994.
- Flores, J., Aldape, F., Diaz, R. V., Hernandez-Mendez, B., and Garcia, R.: PIXE analysis of airborne particulate matter from Xalostoc, Mexico: winter to summer comparison, *Nucl. Instrum. Methods Phys. Res., Sect. B*, 150(1–4), 445–449, 1999.
- Gard, E., Mayer, J. E., Morrical, B. D., Dienes, T., Fergenson, D. P., and Prather, K. A.: Real-time analysis of individual atmospheric aerosol particles: Design and performance of a portable ATOFMS, *Anal. Chem.*, 69(20), 4083–4091, 1997.
- Gross, D. S., Galli, M. E., Kalberer, M., Prevot, A. S. H., Dommen, J., Alfarra, M. R., Duplissy, J., Gaeggeler, K., Gascho, A., Metzger, A., and Baltensperger, U.: Real-time measurement of oligomeric species in secondary organic aerosol with the aerosol time-of-flight mass spectrometer, *Anal. Chem.*, 78(7), 2130–2137, 2006.

Single particle mass spectrometry of Mexico City aerosolsR. C. Moffet

Title Page

Abstract

Introduction

Conclusions

References

Tables

Figures

◀

▶

◀

▶

Back

Close

Full Screen / Esc

Printer-friendly Version

Interactive Discussion

Single particle mass spectrometry of Mexico City aerosols

R. C. Moffet

Title Page

Abstract

Introduction

Conclusions

References

Tables

Figures

◀

▶

◀

▶

Back

Close

Full Screen / Esc

Printer-friendly Version

Interactive Discussion

Gross, D. S., Galli, M. E., Silva, P. J., Wood, S. H., Liu, D. Y., and Prather, K. A.: Single particle characterization of automobile and diesel truck emissions in the Caldecott Tunnel, *Aerosol Sci. Technol.*, 32(2), 152–163, 2000.

Guazzotti, S. A., Coffee, K. R., and Prather, K. A.: Continuous measurements of size-resolved particle chemistry during INDOEX-Intensive Field Phase 99, *J. Geophys. Res. Atmos.*, 106(D22), 28 607–28 627, 2001.

Guazzotti, S. A., Suess, D. T., Coffee, K. R., Quinn, P. K., Bates, T. S., Wisthaler, A., Hansel, A., Ball, W. P., Dickerson, R. R., Neususs, C., Crutzen, P. J., and Prather, K. A.: Characterization of carbonaceous aerosols outflow from India and Arabia: Biomass/biofuel burning and fossil fuel combustion, *J. Geophys. Res. Atmos.*, 108(D15), 4485, doi:10.1029/2002JD003277, 2003.

Hu, C. W., Chao M. R., Wu, K. Y., Chang-Chien, G. P., Lee, W. J., Chang, L. W., and Lee, W. S.: Characterization of multiple airborne particulate metals in the surroundings of a municipal waste incinerator in Taiwan, *Atmos. Environ.*, 37(20), 2845–2852, 2003.

Jacobson, M. Z.: Analysis of aerosol interactions with numerical techniques for solving coagulation, nucleation, condensation, dissolution, and reversible chemistry among multiple size distributions, *J. Geophys. Res. Atmos.*, 107(D19), 4366, doi:10.1029/2001JD002044, 2002.

Jiang, M., Marr, L. C., Dunlea, E. J., Herndon, S. C., Jayne, J. T., Kolb, C. E., Knighton, W. B., Rogers, T. M., Zavala, M., Molina, L. T., and Molina, M. J.: Vehicle fleet emissions of black carbon, polycyclic aromatic hydrocarbons, and other pollutants measured by a mobile laboratory in Mexico City, *Atmos. Chem. Phys.*, 5, 3377–3387, 2005, <http://www.atmos-chem-phys.net/5/3377/2005/>.

Jimenez, J. C., Raga, G. B., Baumgardner, D., Castro, T., Rosas, I., Baez, A., and Morton, O.: On the composition of airborne particles influenced by emissions of the volcano Popocatepetl in Mexico, *Natural Hazards*, 31(1), 21–37, 2004.

Johnson, K. S., de Foy, B., Zuberi, B., Molina, L. T., Molina, M. J., Xie, Y., Laskin, A., and Shutthanandan, V.: Aerosol composition and source apportionment in the Mexico City Metropolitan Area with PIXE/PESA/STIM and multivariate analysis, *Atmos. Chem. Phys.*, 6, 4591–4600, 2006, <http://www.atmos-chem-phys.net/6/4591/2006/>.

Johnson, K. S., Zuberi, B., Molina, L. T., Molina, M. J., Iedema, M. J., Cowin, J. P., Gaspar, D. J., Wang, C., and Laskin, A.: Processing of soot in an urban environment: case study from the Mexico City Metropolitan Area, *Atmos. Chem. Phys.*, 5, 3033–3043, 2005,

<http://www.atmos-chem-phys.net/5/3033/2005/>.

Kanakidou, M., Seinfeld, J. H., Pandis, S. N., Barnes, I., Dentener, F. J., Facchini, M. C., Van Dingenen, R., Ervens, B., Nenes, A., Nielsen, C. J., Swietlicki, E., Putaud, J. P., Balkanski, Y., Fuzzi, S., Horth, J., Moortgat, G. K., Winterhalter, R., Myhre, C. E. L., Tsigaridis, K., Vignati, E., Stephanou, E. G., and Wilson, J.: Organic aerosol and global climate modelling: a review, *Atmos. Chem. Phys.*, 5, 1053–1123, 2005, <http://www.atmos-chem-phys.net/5/1053/2005/>.

Kawamura, K. and Ikushima, K.: Seasonal changes in the distribution of dicarboxylic acids in the urban atmosphere, *Environ. Sci. Technol.*, 27(10), 2227–2235, 1993.

Kawamura, K. and Kaplan, I. R.: Motor exhaust emissions as a primary source for dicarboxylic acids in Los-Angeles ambient air, *Environ. Sci. Technol.*, 21(1), 105–110, 1987.

Krueger, B. J., Grassian, V. H., Cowin, J. P., and Laskin, A.: Heterogeneous chemistry of individual mineral dust particles from different dust source regions: the importance of particle mineralogy, *Atmos. Environ.*, 38(36), 6253–6261, 2004.

Laskin, A., Wietsma, T. W., Krueger, B. J., and Grassian, V. H.: Heterogeneous chemistry of individual mineral dust particles with nitric acid: A combined CCSEM/EDX, ESEM, and ICP-MS study, *J. Geophys. Res. Atmos.*, 110(D10), 10208, doi:10.1029/2004JD005206, 2005.

Liu, D. Y., Wenzel, R. J., and Prather, K. A.: Aerosol time-of-flight mass spectrometry during the Atlanta Supersite Experiment: 1. Measurements, *J. Geophys. Res. Atmos.*, 108(D7), 8426, doi:10.1029/2001JD001562, 2003.

Marr, L. C., Dzepina, K., Jimenez, J. L., Reisen, F., Bethel, H. L., Arey, J., Gaffney, J. S., Marley, N. A., Molina, L. T., and Molina, M. J.: Sources and transformations of particle-bound polycyclic aromatic hydrocarbons in Mexico City, *Atmos. Chem. Phys.*, 6, 1733–1745, 2006,

<http://www.atmos-chem-phys.net/6/1733/2006/>.

Miranda, J., V. A. Barrera, A. A. Espinosa, O. S. Galindo, A. Nunez-Orosco, R. C. Montesinos, A. Leal-Castro, and J. Meinguer: PIXE analysis of atmospheric aerosols from three sites in Mexico City, *Nucl. Instrum. Methods Phys. Res., Sect. B*, 219–20, 157–160, 2004.

Miranda, J., Cahill, T. A., Morales, J. R., Aldape, F., Flores, J., and Diaz, R. V.: Determination of elemental concentrations in atmospheric aerosols in Mexico-City using proton-induced X-Ray emission, proton elastic-scattering, and laser-absorption, *Atmos. Environ.*, 28(14), 2299–2306, 1994.

Miranda, J., Lopez-Suarez, A., Paredes-Gutierrez, R., Gonzalez, S., de Lucio, O. G., Andrade,

Single particle mass spectrometry of Mexico City aerosols

R. C. Moffet

Title Page

Abstract

Introduction

Conclusions

References

Tables

Figures

◀

▶

◀

▶

Back

Close

Full Screen / Esc

Printer-friendly Version

Interactive Discussion

- E., Morales, J. R., and Avila-Sobarzo, M. J.: A study of atmospheric aerosols from five sites in Mexico city using PIXE, Nucl. Instrum. Methods Phys. Res., Sect. B, 137, 970–974, 1998.
- Miranda, J., Morales, J. R., Cahill, T. A., Aldape F., and Flores, J.: A Study of Elemental Contents in Atmospheric Aerosols in Mexico-City, Atmosfera, 5(2), 95–108, 1992.
- 5 Moffet, R. C. and Prather, K. A.: Extending ATOFMS measurements to include refractive index and density, Anal. Chem., 77(20), 6535–6541, 2005.
- Molina, L. T. and Molina, M. J.: Air Quality in the Mexico Megacity: An Integrated Assessment, Kluwer Academic Publishers, Boston, 1–384, 2002.
- Morawska, L. and Zhang, J. F.: Combustion sources of particles. 1. Health relevance and
10 source signatures, Chemosphere, 49(9), 1045–1058, 2002.
- Moya, M., Ansari, A. S., and Pandis, S. N.: Partitioning of nitrate and ammonium between the gas and particulate phases during the 1997 IMADA-AVER study in Mexico City, Atmos. Environ., 35(10), 1791–1804, 2001.
- Moya, M., Castro, T., Zepeda, M., and Baez, A.: Characterization of size-differentiated inorganic composition of aerosols in Mexico City, Atmos. Environ., 37(25), 3581–3591, 2003.
- 15 Moya, M., Grutter, M., and Baez, A.: Diurnal variability of size-differentiated inorganic aerosols and their gas-phase precursors during January and February of 2003 near downtown Mexico City, Atmos. Environ., 38(33), 5651–5661, 2004.
- Mugica, V., Maubert, M., Torres, M., Munoz, J., and Rico, E.: Temporal and spatial variations
20 of metal content in TSP and PM10 in Mexico City during 1996–1998, J. Aerosol Sci., 33(1), 91–102, 2002.
- Noble, C. A. and Prather, K. A.: Real-time measurement of correlated size and composition profiles of individual atmospheric aerosol particles, Environ. Sci. Technol., 30(9), 2667–2680, 1996.
- 25 Olmez, I., Sheffield, A. E., Gordon, G. E., Houck, J. E., Pritchett, L. C., Cooper, J. A., Dzubay, T. G., and Bennett, R. L.: Compositions of particles from selected sources in philadelphia for receptor modeling applications, JAPCA-the International Journal of Air Pollution Control and Hazardous Waste Management, 38(11), 1392–1402, 1988.
- Ondov, J. M. and Wexler, A. S.: Where do particulate toxins reside? An improved paradigm for
30 the structure and dynamics of the urban mid-Atlantic aerosol, Environ. Sci. Technol., 32(17), 2547–2555, 1998.
- Pastor, S. H., Allen, J. O., Hughes, L. S., Bhave, P., Cass, G. R., and Prather, K. A.: Ambient single particle analysis in Riverside, California by aerosol time-of-flight mass spectrometry

Single particle mass spectrometry of Mexico City aerosolsR. C. Moffet

[Title Page](#)[Abstract](#)[Introduction](#)[Conclusions](#)[References](#)[Tables](#)[Figures](#)[◀](#)[▶](#)[◀](#)[▶](#)[Back](#)[Close](#)[Full Screen / Esc](#)[Printer-friendly Version](#)[Interactive Discussion](#)

Single particle mass spectrometry of Mexico City aerosols

R. C. Moffet

Title Page

Abstract

Introduction

Conclusions

References

Tables

Figures

◀

▶

◀

▶

Back

Close

Full Screen / Esc

Printer-friendly Version

Interactive Discussion

during the SCOS97-NARSTO, Atmos. Environ., 37, S239–S258, 2003.

Pitts, J. N., Grosjean, D., Vancauwenberghe, K., Schmid, J. P., and Fitz, D. R.: Photo-oxidation of aliphatic-amines under simulated atmospheric conditions - formation of nitrosamines, nitramines, amides, and photo-chemical oxidant, Environ. Sci. Technol., 12(8), 946–953, 1978.

Qin, X. Y., Bhave, P. V., and Prather, K. A.: Comparison of two methods for obtaining quantitative mass concentrations from aerosol time-of-flight mass spectrometry measurements, Anal. Chem., 78(17), 6169–6178, 2006.

Qin, X. Y. and Prather, K. A.: Impact of biomass emissions on particle chemistry during the California Regional Particulate Air Quality Study, Int. J. Mass Spectrom., 258 (1–3), 142–150, 2006.

Raga, G. B., Baumgardner, D., Castro, T., Martinez-Arroyo, A., and Navarro-Gonzalez, R.: Mexico City air quality: a qualitative review of gas and aerosol measurements (1960–2000), Atmos. Environ., 35(23), 4041–4058, 2001.

Salcedo, D., Onasch, T. B., Dzepina, K., Canagaratna, M. R., Zhang, Q., Huffman, J. A., DeCarlo, P. F., Jayne, J. T., Mortimer, P., Worsnop, D. R., Kolb, C. E., Johnson, K. S., Zuberi, B., Marr, L. C., Volkamer, R., Molina, L. T., Molina, M. J., Cardenas, B., Bernabe, R. M., Marquez, C., Gaffney, J. S., Marley, N. A., Laskin, A., Shutthanandan, V., Xie, Y., Brune, W., Leshner, R., Shirley, T., and Jimenez, J. L.: Characterization of ambient aerosols in Mexico City during the MCMA-2003 campaign with Aerosol Mass Spectrometry: results from the CENICA Supersite, Atmos. Chem. Phys., 6, 925–946, 2006, <http://www.atmos-chem-phys.net/6/925/2006/>.

Schlesinger, W. H. and Hartley, A. E.: A Global Budget for Atmospheric NH₃, Biogeochemistry, 15(3), 191–211, 1992.

Seibert, P., Kromp-Kolb, H., Baltensperger, U., Jost, D. T., and Schwikowski, M.: Trajectory analysis of high-alpine air pollution data, in, Plenum Press, New York, 1994.

Silva, P. J., Liu, D. Y., Noble, C. A., and Prather, K. A.: Size and chemical characterization of individual particles resulting from biomass burning of local Southern California species, Environ. Sci. Technol., 33(18), 3068–3076, 1999.

Silva, P. J. and Prather, K. A.: Source profiling and apportionment of airborne particles: A new approach using aerosol time-of-flight mass spectrometry, University of California, Riverside, Riverside, 189–208, 2000.

Sodeman, D. A., Toner, S. M., and Prather, K. A.: Determination of single particle mass spec-

tral signatures from light-duty vehicle emissions, *Environ. Sci. Technol.*, 39(12), 4569–4580, 2005.

Song, X. H., Hopke, P. K., Fergenson, D. P., and Prather, K. A.: Classification of single particles analyzed by ATOFMS using an artificial neural network, *ART-2A, Anal. Chem.*, 71(4), 860–865, 1999.

Stohl, A., Forster, C., Frank, A., Seibert, P., and Wotawa, G.: Technical note: The Lagrangian particle dispersion model FLEXPART version 6.2, *Atmos. Chem. Phys.*, 5, 2461–2474, 2005, <http://www.atmos-chem-phys.net/5/2461/2005/>.

Suarez, A. E. and Ondov, J. M.: Ambient aerosol concentrations of elements resolved by size and by source: Contributions of some cytokine-active metals from coal- and oil-fired power plants, *Energy and Fuels*, 16(3), 562–568, 2002.

Sullivan, R. C., Guazzotti, S. A., Sodeman, D. A., and Prather, K. A.: Direct observations of the atmospheric processing of Asian mineral Dust, *Atmos. Chem. Phys.*, 7, 1213–1236, 2007, <http://www.atmos-chem-phys.net/7/1213/2007/>.

Tolocka, M. P., Lake, D. A., Johnston, M. V., and Wexler, A. S.: Number concentrations of fine and ultrafine particles containing metals, *Atmos. Environ.*, 38(20), 3263–3273, 2004.

Toner, S. M., Sodeman, D. A., and Prather, K. A.: Single particle characterization of ultrafine and accumulation mode particles from heavy duty diesel vehicles using aerosol time-of-flight mass spectrometry, *Environ. Sci. Technol.*, 40(12), 3912–3921, 2006.

Vega, E., Mugica, V., Reyes, E., Sanchez, G., Chow, J. C., and Watson, J. G.: Chemical composition of fugitive dust emitters in Mexico City, *Atmos. Environ.*, 35(23), 4033–4039, 2001.

Vega, E., Reyes, E., Sanchez, G., Ortiz, E., Ruiz, M., Chow, J., Watson, J., and Edgerton, S.: Basic statistics of PM_{2.5} and PM₁₀ in the atmosphere of Mexico city, *Sci. Total Environ.*, 287(3), 167–176, 2002.

Wenzel, R. J., Liu, D. Y., Edgerton, E. S., and Prather, K. A.: Aerosol time-of-flight mass spectrometry during the Atlanta Supersite Experiment: 2. Scaling procedures, *J. Geophys. Res. Atmos.*, 108(D7), 8424, doi:10.1029/2001JD001563, 2003.

Yao, X. H., Fang, M., and Chan, C. K.: Size distributions and formation of dicarboxylic acids in atmospheric particles, *Atmos. Environ.*, 36(13), 2099–2107, 2002.

ACPD

7, 6413–6457, 2007

Single particle mass spectrometry of Mexico City aerosols

R. C. Moffet

Title Page

Abstract

Introduction

Conclusions

References

Tables

Figures

◀

▶

◀

▶

Back

Close

Full Screen / Esc

Printer-friendly Version

Interactive Discussion

Single particle mass spectrometry of Mexico City aerosols

R. C. Moffet

Table 1. Peak searching criteria for secondary species.

Secondary Marker	m/z
NH ₄	+18
NO ₂	-46
NO ₃	-62
SO ₃	-80
HSO ₄	-97
C ₂ O ₃ OH	-89
C ₂ H ₃ O	+43

[Title Page](#)[Abstract](#)[Introduction](#)[Conclusions](#)[References](#)[Tables](#)[Figures](#)[I◀](#)[▶I](#)[◀](#)[▶](#)[Back](#)[Close](#)[Full Screen / Esc](#)[Printer-friendly Version](#)[Interactive Discussion](#)

Single particle mass spectrometry of Mexico City aerosols

R. C. Moffet

Title Page

Abstract

Introduction

Conclusions

References

Tables

Figures

◀

▶

◀

▶

Back

Close

Full Screen / Esc

Printer-friendly Version

Interactive Discussion

Table 2. Peak searching criteria for primary species.

Primary Species	Marker	m/z	Logical
C	C	12	
Cl	Cl	–35	
PO ₃	PO ₃	–79	
Na	Na	23	
K	K	39	
NaKCl	Na	23	
	K	39	And
	Cl	–35	And
NaCl only	Na	23	
	Cl	–35	And
	K	39	AndNot
Zn not Pb	Zn	64	
	Zn	66	And
	Pb	206–209	AndNot
CaEC	C ₃	36	
	C ₄	48	And
	C ₅	60	And
	Ca	40	And
Ca	Ca	40	

Single particle mass spectrometry of Mexico City aerosols

R. C. Moffet

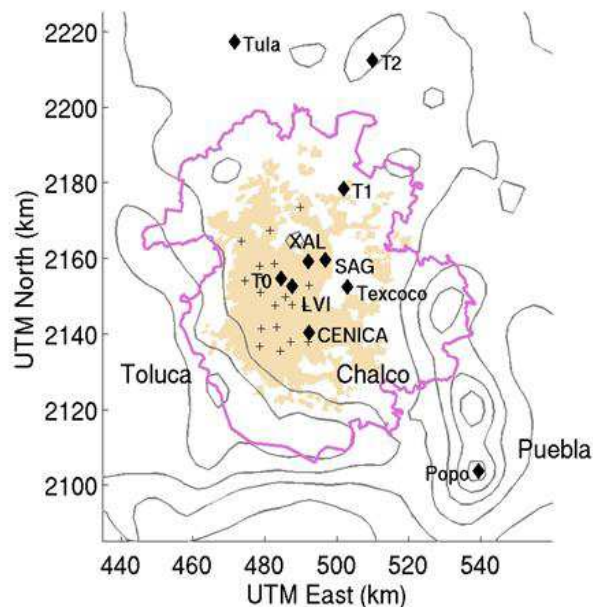


Fig. 1. A map of the Mexico City Metropolitan Area (MCMA). The sampling site these measurements were carried out at was called T0, and was located at the Instituto Mexicano Del Petroleo (IMP). RAMA sites are shown as the + symbol. The political border of the MCMA as of 2003 is in pink and urban area as of 1995 are in beige. Terrain contours are every 500 m.

[Title Page](#)[Abstract](#)[Introduction](#)[Conclusions](#)[References](#)[Tables](#)[Figures](#)[◀](#)[▶](#)[◀](#)[▶](#)[Back](#)[Close](#)[Full Screen / Esc](#)[Printer-friendly Version](#)[Interactive Discussion](#)

Single particle mass spectrometry of Mexico City aerosols

R. C. Moffet

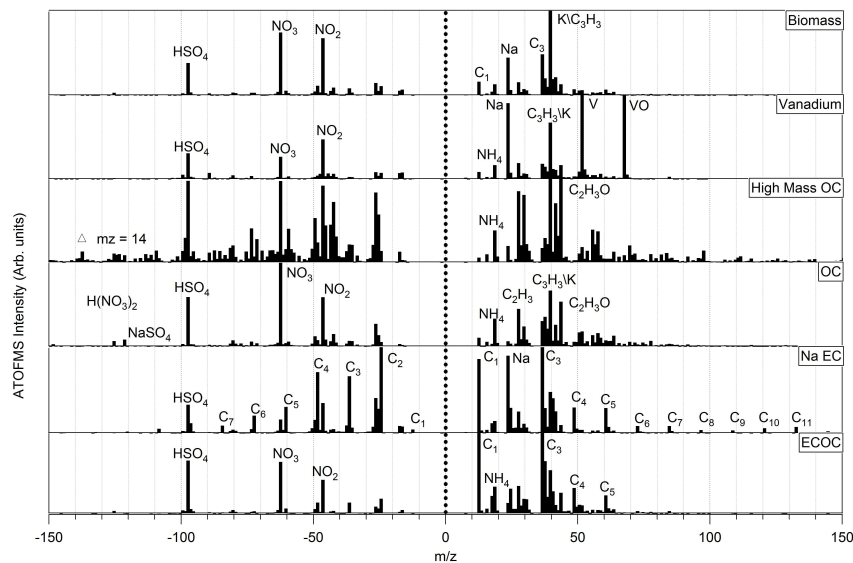


Fig. 2a. Average spectra of single particle types as determined with the ART-2a clustering algorithm. The particle types shown here occurred mainly in the submicron portion of the size distribution.

[Title Page](#)[Abstract](#)[Introduction](#)[Conclusions](#)[References](#)[Tables](#)[Figures](#)[◀](#)[▶](#)[◀](#)[▶](#)[Back](#)[Close](#)[Full Screen / Esc](#)[Printer-friendly Version](#)[Interactive Discussion](#)

Single particle mass spectrometry of Mexico City aerosols

R. C. Moffet

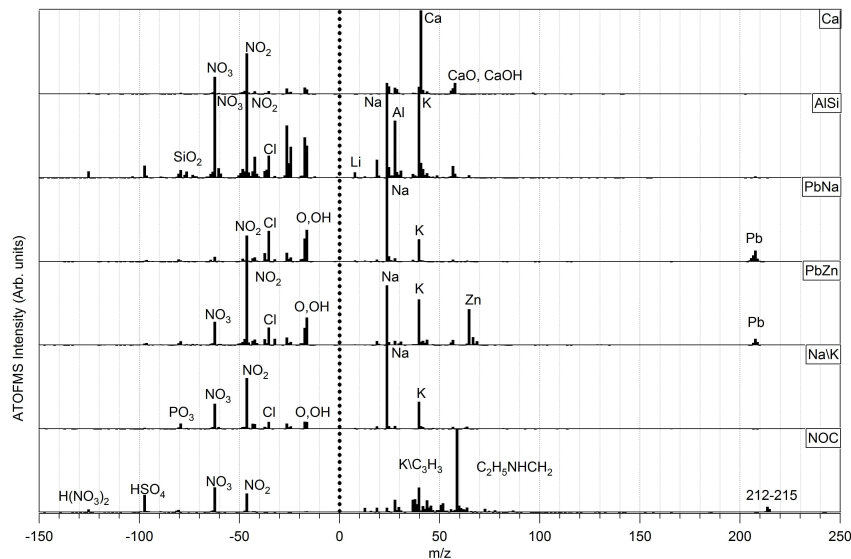


Fig. 2b. Average spectra of single particle types as determined with the ART-2a clustering algorithm. The m/z range is extended to 250Da compared to Fig. 2a to show important peaks such as Pb for the industrial types and the unknown markers at 212–215 for the NOC type. Common coarse mode particle types shown here include: Ca, AlSi and Na/K. NOC was primarily of submicron sizes.

Title Page

Abstract

Introduction

Conclusions

References

Tables

Figures

◀

▶

◀

▶

Back

Close

Full Screen / Esc

Printer-friendly Version

Interactive Discussion

Single particle mass spectrometry of Mexico City aerosols

R. C. Moffet

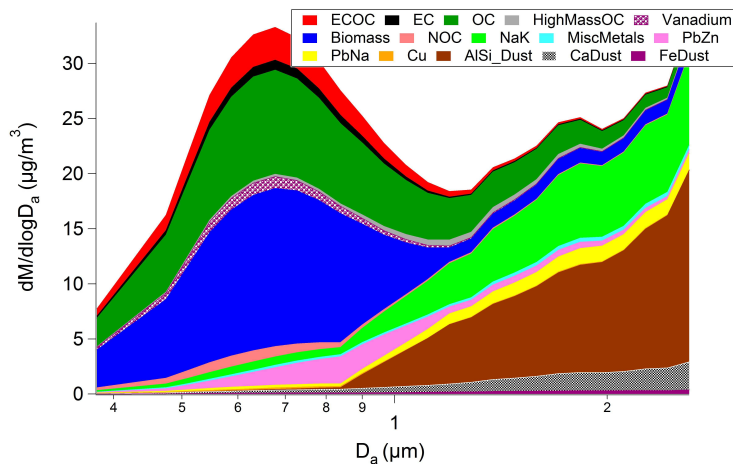


Fig. 3. Average scaled PM_{2.5} mass distribution, showing the contribution of the single particle types for the MCMA – 2006 campaign. The individual distributions are stacked upon one another.

Title Page

Abstract

Introduction

Conclusions

References

Tables

Figures

◀

▶

◀

▶

Back

Close

Full Screen / Esc

Printer-friendly Version

Interactive Discussion

Single particle mass spectrometry of Mexico City aerosols

R. C. Moffet

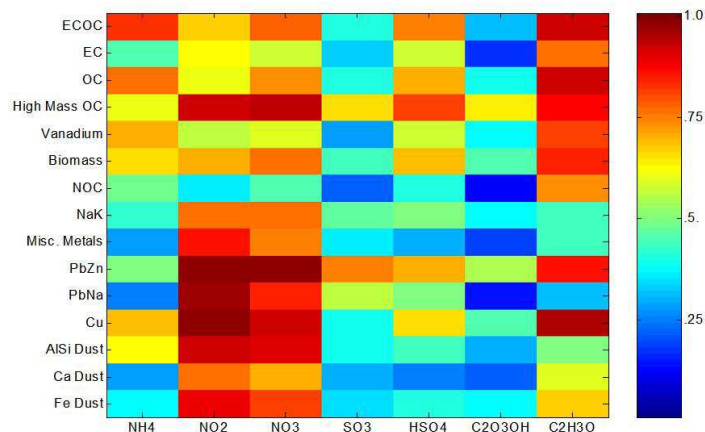


Fig. 4. Mixing state of secondary species on the various single particle types. The secondary species were identified by the peak searching criteria described in Table 1. The peak searches were applied to the entire dataset and then intersected with the particle classes. The color scale represents the fraction of particles within a single particle type (y-axis) that contain the secondary species (x-axis).

[Title Page](#)[Abstract](#)[Introduction](#)[Conclusions](#)[References](#)[Tables](#)[Figures](#)[◀](#)[▶](#)[◀](#)[▶](#)[Back](#)[Close](#)[Full Screen / Esc](#)[Printer-friendly Version](#)[Interactive Discussion](#)

Single particle mass spectrometry of Mexico City aerosols

R. C. Moffet

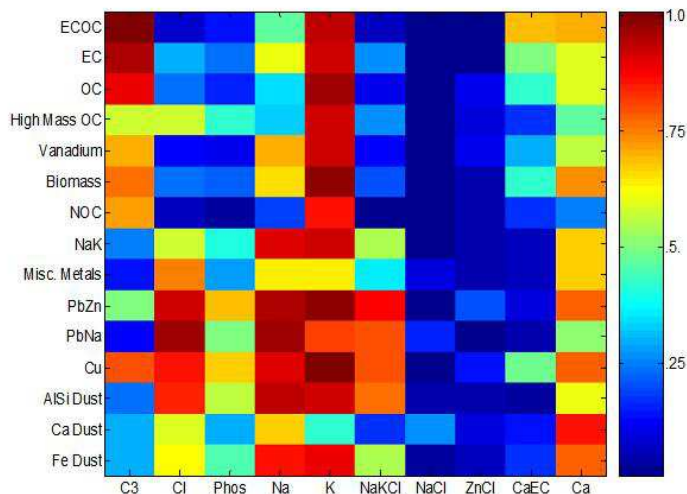


Fig. 5. Mixing state of primary species on the various single particle types. The primary species were identified by the peak searching criteria described in Table 2. The peak searches were applied to the entire dataset and then intersected with the particle classes. The color scale represents the fraction of particles within a single particle type (y-axis) that contain the primary species (x-axis).

[Title Page](#)[Abstract](#)[Introduction](#)[Conclusions](#)[References](#)[Tables](#)[Figures](#)[◀](#)[▶](#)[◀](#)[▶](#)[Back](#)[Close](#)[Full Screen / Esc](#)[Printer-friendly Version](#)[Interactive Discussion](#)

Single particle mass spectrometry of Mexico City aerosols

R. C. Moffet

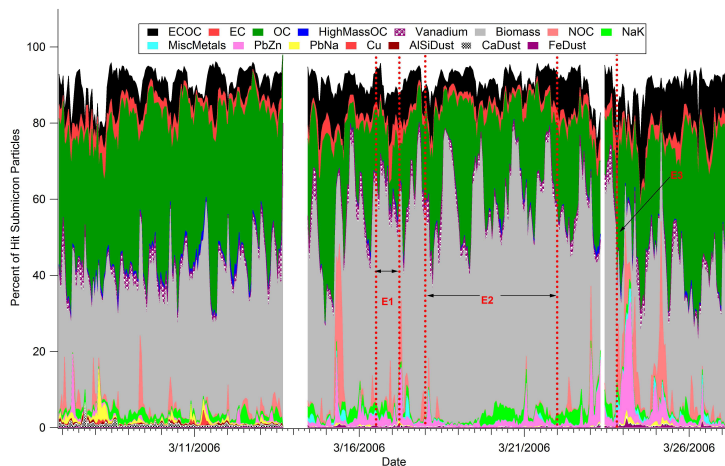


Fig. 6a. Temporal of the submicron particle types during MCMA-2006.

Title Page

Abstract

Introduction

Conclusions

References

Tables

Figures

◀

▶

◀

▶

Back

Close

Full Screen / Esc

Printer-friendly Version

Interactive Discussion

Single particle mass spectrometry of Mexico City aerosols

R. C. Moffet

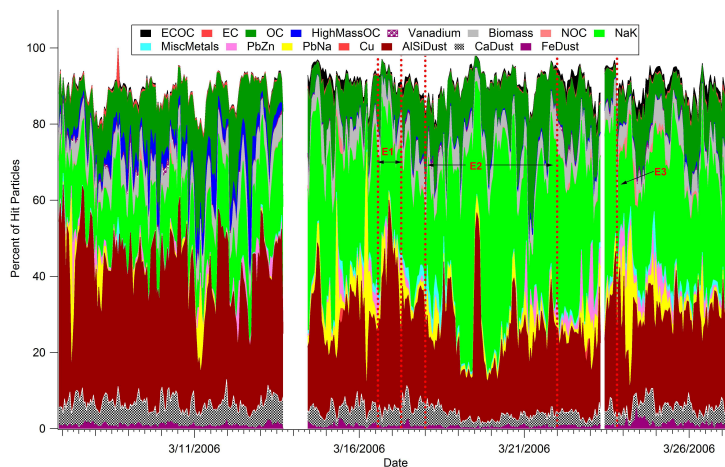


Fig. 6b. Temporal of the supermicron particle types during MCMA-2006.

Title Page

Abstract

Introduction

Conclusions

References

Tables

Figures

◀

▶

◀

▶

Back

Close

Full Screen / Esc

Printer-friendly Version

Interactive Discussion

Single particle mass spectrometry of Mexico City aerosols

R. C. Moffet

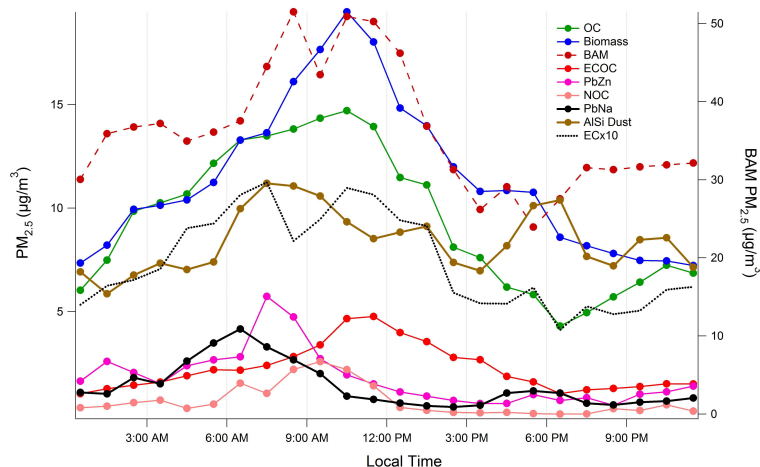


Fig. 7. Average diurnal cycle of selected types. The ATOFMS scaled mass concentration is shown on the left axis and the mass concentration derived from the Beta Attenuation Monitor (BAM) is shown on the right axis for comparison.

[Title Page](#)[Abstract](#)[Introduction](#)[Conclusions](#)[References](#)[Tables](#)[Figures](#)[◀](#)[▶](#)[◀](#)[▶](#)[Back](#)[Close](#)[Full Screen / Esc](#)[Printer-friendly Version](#)[Interactive Discussion](#)

Single particle mass spectrometry of Mexico City aerosols

R. C. Moffet

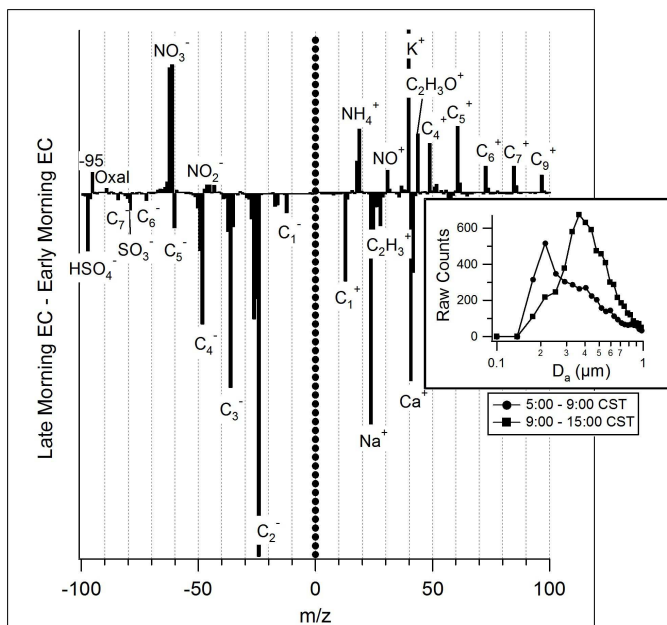


Fig. 8. A subtraction spectrum for EC particles peaking later in the morning (9a–3p) minus particles peaking early in the morning (5–9a). This shows that early morning EC particles have less contribution from markers of secondary photochemistry and more markers from freshly emitted EC (sulfate, Na^+ , and Ca^+). Furthermore, the increase in K^+ later in the day suggests a contribution from a different primary source of EC or ageing by coagulation.

Title Page

Abstract

Introduction

Conclusions

References

Tables

Figures

◀

▶

◀

▶

Back

Close

Full Screen / Esc

Printer-friendly Version

Interactive Discussion

Single particle mass spectrometry of Mexico City aerosols

R. C. Moffet

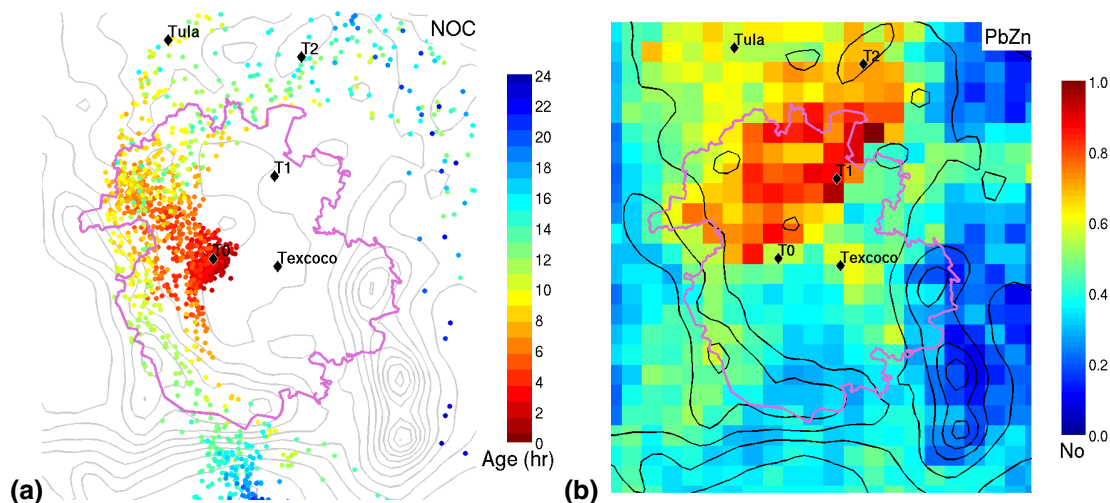


Fig. 9. Spatial distributions of industrial emissions in Mexico City. **(a)** Particle back-trajectories for a release on 15 March, 08:00–09:00 CST, for a representative nitrogen containing organic carbon (NOC) peak. Particle positions are plotted every hour and color indicates age. **(b)** Concentration field analysis for PbZn particles. High non-dimensional number (red) indicates possible source regions, low numbers (blue) indicate areas with low or zero emissions.

[Title Page](#)[Abstract](#)[Introduction](#)[Conclusions](#)[References](#)[Tables](#)[Figures](#)[◀](#)[▶](#)[◀](#)[▶](#)[Back](#)[Close](#)[Full Screen / Esc](#)[Printer-friendly Version](#)[Interactive Discussion](#)

Single particle mass spectrometry of Mexico City aerosols

R. C. Moffet

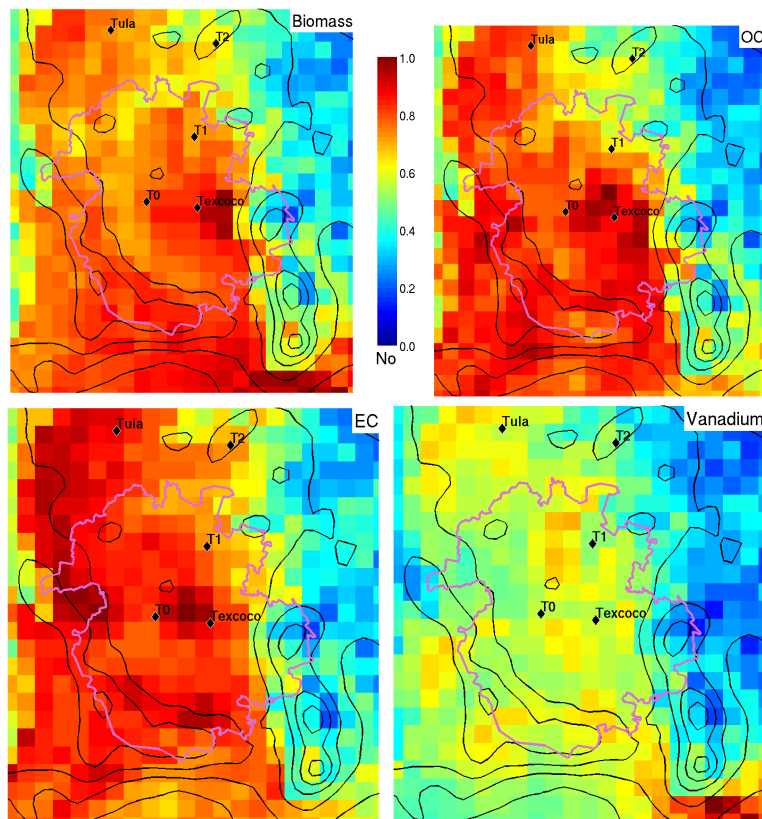


Fig. 10. Concentration field analysis for select carbonaceous particle types. High non-dimensional number (red) indicates possible source regions, low numbers (blue) indicate areas with low emissions.

[Title Page](#)[Abstract](#)[Introduction](#)[Conclusions](#)[References](#)[Tables](#)[Figures](#)[◀](#)[▶](#)[◀](#)[▶](#)[Back](#)[Close](#)[Full Screen / Esc](#)[Printer-friendly Version](#)[Interactive Discussion](#)

Single particle mass spectrometry of Mexico City aerosols

R. C. Moffet

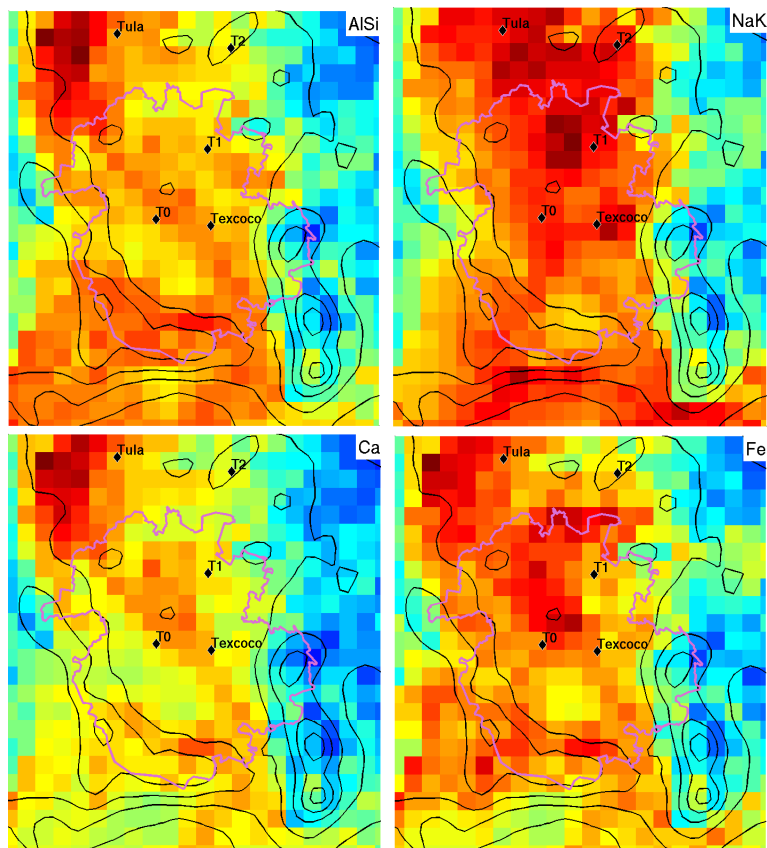


Fig. 11. Concentration field analysis for select coarse mode particle types. High non-dimensional number (red) indicates possible source regions, low numbers (blue) indicate areas with low or zero emissions.

[Title Page](#)[Abstract](#)[Introduction](#)[Conclusions](#)[References](#)[Tables](#)[Figures](#)[◀](#)[▶](#)[◀](#)[▶](#)[Back](#)[Close](#)[Full Screen / Esc](#)[Printer-friendly Version](#)[Interactive Discussion](#)